

Characterization of Wet Powder-Sprayed Zirconia/Calcium Phosphate Coating for Dental Implants

Karoline Pardun, Dipl. Biol.;* Laura Treccani, Dr. rer. nat;† Eike Volkmann, MSc;‡ Giovanni Li Destri, PhD;§ Giovanni Marletta, MSc;¶ Philipp Streckbein, MD, DDS;*** Christian Heiss, MD, PhD;†† Kurosch Rezwan, Dr. Ing**

ABSTRACT

Purpose: Yttria-stabilized zirconia (TZ) is used for dental applications because of its low toxicity and beneficial mechanical properties, but it does not stimulate bone regeneration around the implant due to its bioinertness. Therefore, hydroxyapatite (HA) coatings are often utilized to increase the surface bioactivity and to achieve a better osseointegration. These coatings, however, are chemically nonstable and provide a weak bonding to the substrate surface.

Materials and Methods: In this study, zirconia substrates were coated with a calcium phosphate/zirconia mixture to achieve ceramic coatings with a high bioactivity potential and a good mechanical stability. The coatings were obtained by wet powder spraying (WPS). Pure HA and TZ coatings were employed as reference materials. The coatings were characterized with regard to microstructure, surface roughness, and phase composition. Scratch tests were carried out to investigate the coating adhesion. The influence of the coating on the mechanical strength was evaluated with the ball on three balls test (B3B). In addition, zirconia dental implant screws were also coated and inserted in a biomechanical test block and bovine rib bone.

Results: After sintering, the mixed coating exhibited a porous morphology with a surface roughness of about 4 μm and a total porosity of 17%. Phase analysis showed a transformation from TZ and HA to calcium zirconium oxide and tricalcium phosphate. Investigations of the bond strength confirmed a strong adhesion of the mixed coating to the substrate, while the biaxial fracture strength was only slightly affected. Insertion experiments confirmed the scratch test results and evidenced an intact mixed coating on the zirconia screw.

Conclusions: The present study revealed a higher stability and firm adhesion of the mixed coating compared with a pure calcium phosphate coating. We also successfully demonstrate the particular versatility of the WPS technique for dental implants by coating a complex curved surface.

KEY WORDS: coating adhesion, dental implants, hydroxyapatite, wet powder spraying, zirconia

*Research associate, Advanced Ceramics, University of Bremen, Bremen, Germany; †senior scientist, Advanced Ceramics, University of Bremen, Bremen, Germany; ‡research associate, Advanced Ceramics, University of Bremen, Bremen, Germany; §postdoctoral researcher, Department of Chemical Sciences, University of Catania, Catania, Italy; ¶professor, Department of Chemical Sciences, University of Catania, Catania, Italy; **senior consultant, Department of Cranio-Maxillo-Facial Surgery, University Hospital, Justus-Liebig-University Giessen, Giessen, Germany; ††vice head, Department of Trauma Surgery, University Hospital of Giessen-Marburg, Giessen, Germany, and Laboratory of Experimental Surgery, Giessen, Germany; ***professor, Advanced Ceramics, University of Bremen, Bremen, Germany

Reprint requests: Prof. Kurosch Rezwan, Advanced Ceramics, University of Bremen, Am Biologischen Garten 2, 28359 Bremen, Germany; e-mail: krezwan@uni-bremen.de

The authors declare no conflicts of interest

© 2013 Wiley Periodicals, Inc.

DOI 10.1111/cid.12071

INTRODUCTION

The material surface features and composition of orthopedic and dental implants play a crucial role for proper bone tissue interaction. Today, titanium or titanium alloys represent standard materials for dental applications because of their biocompatibility and favorable mechanical properties.¹ Yttria-stabilized zirconia (TZ), on the other hand, is used in the biomedical field due to its low toxicity and beneficial mechanical properties, like high bending strength, fracture toughness, and hardness, compared with metals and other ceramics. Although TZ is known for its good biocompatibility, it does not stimulate extensive bone regeneration around the implant because of its bioinertness.²⁻⁷ However, lack of material integration in the surrounding bone can

cause the formation of connective tissue that in turn induces a premature loosening of the implant.⁸ During the past two decades, different surface modification strategies have been investigated to enhance the contact at the bone-implant interface, for example, sand-blasting,⁹ laser treatment,^{10,11} or by creating surface coatings featuring specific composition, topography, and roughness.^{12,13}

Calcium phosphate-based materials, such as hydroxyapatite (HA) or tricalcium phosphate (TCP), are widely used as coatings.^{14–16} These calcium phosphates (CP) are known to be osteoconductive and resorbable to some extent.¹⁷ In vitro investigations have shown an improved adhesion and proliferation of osteoblasts to CP-coated titania and TZ, while in vivo a significantly improved tissue integration could be detected.^{18,19} Although this approach is effective, for example, for increasing the bioactivity of the implant surface, it suffers from several drawbacks. In particular, these coatings are poorly stable and provide a weak bonding to the substrate.^{20–23} The detachment of the coating can lead to defects at the bone-implant interface and provoke the loss of the implant, even if initially a good adhesion between the coating and the surrounding bone tissue existed. Therefore, several studies have been done so far with TZ reinforced HA composites and coatings to combine enhanced mechanical properties with an improved osseointegration. Previous research indicated that the addition of TZ as second phase to HA causes a significant increase of coating hardness and adhesive strength. Furthermore, it could be shown that TZ/HA coatings are not cytotoxic and enhance cell attachment and proliferation.^{24,25} Most of the implemented studies have been done with titanium, titanium alloys, and stainless steel substrates. Only very little has been conducted up to now about the surface modification of zirconia substrates with TZ reinforced HA coatings for dental applications.

For the coating of metals and ceramic substrates, numerous methods have been developed. The most commonly used methods include plasma spraying^{26,27} and sol-gel technology,^{14,28} each with different advantages and disadvantages. Plasma-sprayed coatings possess a thickness of a few microns to a few millimeters and are not appropriate for complex-shaped parts like dental implants.¹³ Whereas coatings obtained by sol-gel method are relatively homogeneous but can only be produced crack free within a thickness of 0.1 to 1 μm .²⁹

This study presents the deposition of a mixed coating on TZ using wet powder spraying (WPS).^{30–32} The sprayed suspension consists of HA and TZ to provide a partially resorbable part (HA) and at the same time a nonresorbable part (TZ) of sufficient strength for a better adhesion of the coating to the substrate. Therefore, the mechanical stability and coating adhesion are studied, as well as the chemical composition. In addition, the suitability of the WPS technique to fabricate uniform coatings on geometrically complex-shaped parts is also investigated.

MATERIALS AND METHODS

Substrate Preparation

The substrates used in this study were prepared from commercially available TZ-3YSB-E powder (Tosoh, Tokyo, Japan) by uniaxially dry pressing (Weber Maschinen- und Apparatebau GmbH, Remshalden, Germany) in a cylindrical form (20 mm diameter) with a force of 12 kN. The substrates were afterward isostatically densified in a cold isostatic press (aad Hochdrucktechnik, Bad Homburg, Germany) at 1,200 bar for 5 minutes and subsequently presintered at 1,100°C for 2 hours (LHT08/17, Nabertherm GmbH, Lilienthal, Germany). Zirconia dental implants (l = 17 mm, \varnothing = 4.5 mm, INMAFEED K1012, INMATEC Technologies GmbH, Rheinbach, Germany) were manufactured according to a modified geometry design provided by an implant manufacturer (BEGO Implant Systems, Bremen, Germany) via injection molding and presintered at 950°C for 2 hours (Fraunhofer IFAM, Bremen, Germany).

Suspension Preparation

The suspension to coat the presintered zirconia substrates were produced from TZ-3YS-E (TZ, Tosoh) and HA powder (Sigma Aldrich Chemie GmbH, Munich, Germany). The characteristics of the used powders are given in Table 1. The aqueous ceramic suspension

TABLE 1 Characteristics of TZ and HA Powders Used for Suspension Preparation

Particle Size (d_{50} , nm)	Isoelectric Point	Specific Surface (m^2/g)	Density (g/cm^3)
360 ± 0.37	8.5	7.0 ± 2.0	6.05
151 ± 0.24	6.9	58.2 ± 0.1	3.15

consisted of 7.5 vol. % HA and 7.5 vol. % TZ. The ceramic suspension was stabilized at pH 10 by the addition of ammonium hydroxide solution (25% NH_3 basis, Sigma Aldrich) to prevent particle agglomeration. Additionally, a polyacrylic acid-based (PAA) dispersant was added (12 mg/g ceramic powder, Syntran® 8220, Interpolymer GmbH, Hassloch, Germany) for electrosteric stabilization. As reference materials, pure HA and TZ coatings were used, for which water-based suspensions were prepared with solid contents of 12 vol. % for HA and 20 vol. % for TZ, respectively. Both suspensions were stabilized with PAA. The HA suspension was adjusted to pH 10 and TZ to pH 6 with ammonia solution. The dissolution of potential agglomerates in the prepared ceramic suspensions was achieved by ultrasonic homogenization (Sonifier 450, Branson, Dietzenbach, Germany) for 10 minutes (mixed and pure TZ suspension) and 3 minutes (pure HA suspension). The compositions of the different coatings are summarized in Table 2.

WPS

The presintered zirconia substrates (diameter: 15 mm, height: 1.7 mm) were coated via WPS. A schematic diagram of the WPS is shown in Figure 1. The coating was carried out with a double-action airbrush spray gun (BD 183-K, Artistic Life, Boenen, Germany). During the spraying process, the airbrush was moved from top to bottom with a speed of 1 cm/s. The spraying parameters are listed below and kept constant for all suspensions:

Spraying distance: 200 mm

Air pressure: 2 bar

Airbrush nozzle: 0.8 mm

Relative humidity: ~60%

Spraying time: 3 s

TABLE 2 Composition of the Sprayed Coatings and Suspension Deposition Rate

Sample Name	Substrate	Coating	Suspension Deposition Rate
CP	TZ	12 vol.% HA	15.9 ± 1.9 g/min
TZ	TZ	20 vol.% TZ	7.4 ± 1.6 g/min
TZCP	TZ	7.5 vol.% TZ 7.5 vol.% HA	9.3 ± 1.7 g/min

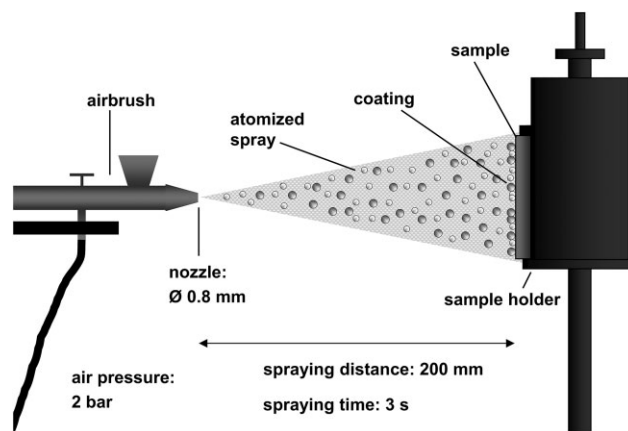


Figure 1 Experimental setup of the wet powder spraying (WPS) process. The coating was applied with a double-action airbrush from a distance of 200 mm and with an air pressure of 2 bar. Airbrush nozzle diameter: 0.8 mm.

The deposition rates of different coatings are listed in Table 2. The coated samples were dried for 24 hours under ambient conditions and subsequently sintered at 1,500°C for 2 hours.

Coating Characterization

The resulting microstructure of the coatings was studied after sintering using scanning electron microscopy (SEM; Camscan Series 2, Obducat CamScan Ltd, Cambridgeshire, UK). The samples were sputter coated with gold for 60 s before examination (K550, Emitech, West Sussex, UK), and images were taken at 20 kV using secondary electron mode.

The surface roughness of the different coatings was analyzed using an optical profilometer (Plu2300, Sensofar, Terrassa, Spain) by scanning a surface area of $477 \times 636 \mu\text{m}^2$. The measurements were done in triplicates on 15 different samples for each coating. The average surface roughness (S_a) were calculated according to ISO25178. This standard deals with the analysis of areal surface roughness and covers the noncontact measurements carried out with optical profilometry.

The characterization of the coating thickness, pore size, and total porosity was done by image analysis (Image J 1.42q, National Institute of Health, Bethesda, MD, USA) of representative top views and cross-sections.

Energy-dispersive X-ray spectroscopy (EDX) mapping was carried out with an INCA PentalFETx3 (Oxford Instruments, Tubney Woods, UK) mounted to a SEM Supra40 (Carl Zeiss AG, Oberkochen, Germany). The mapping was done from the top view and a polished

resin embedded cross-section (EpoFix, Struers GmbH, Willich, Germany) of the mixed coating. The samples were sputter coated with carbon for 9 s with a Carbon Coater 108 (Cressington, Watford, UK).

The phase composition of the coatings was examined, after sintering, by Grazing Incidence X-ray Diffraction (GI-XRD) using an Ultima IV type III diffractometer (Rigaku, Tokyo, Japan) equipped with Cross Beam Optics by using a $K\alpha$ wavelength emitted by a Cu anode. Careful alignment of source and detector with respect to the sample was reached by using a thin film attachment with three degrees of freedom. In order to avoid beam defocusing, the measurements were carried out in parallel beam mode. Divergence of the primary beam was reduced by a 5° Soller slit, while divergence of the diffracted beam was reduced by a 0.5° horizontal Soller slit. The incident angle was kept at 0.5° . In order to identify the phase composition of each sample, a Rietveld refinement was performed using, as a reference, the powder patterns stored in the database of the International Centre of Diffraction Data (Newtown Square, PA, USA). In particular, the PDXL software licensed by Rigaku was employed to minimize the difference between experimental and calculated data.

Characterization of Mechanical Properties

Scratch tests were performed with a pencil hardness tester (PH-5800, BYK-Gardner GmbH, Geretsried, Germany) according to ISO15184. The test was carried out with a pencil (Vickers hardness 90.6 ± 2.5 HV 0.2) and a sharpened bovine femur (Vickers hardness 89.8 ± 5.2 HV 0.2), which was previously ground into a pencil shape. The pencil or the bone were fixed in a sclerometer and moved over the surface with a load of 7.5 N and a velocity of 1 mm/s for a distance of 12 mm. Carbon and bone leftovers on the sample surface were burned out at $1,000^\circ\text{C}$ and $1,400^\circ\text{C}$ after the test, respectively, and the sample surface was examined with SEM.

The influence of the coating on the mechanical strength of the substrate material was tested with the ball on three balls (B3B) biaxial flexural test performed on a universal testing machine (Zwick/Roell Z005, Ulm, Germany) with balls of 4 mm radius and a test speed of 0.5 mm/min. Thirty samples were tested for each coating, and the fracture strength was calculated with the following Eq. 1:

$$\sigma_{\max} = \frac{3 \cdot F \cdot (1 + \nu)}{4 \cdot \pi \cdot t^2} \cdot \left[1 + 2 \ln \left(\frac{Ra}{t/3} \right) + \frac{1 - \nu}{1 + \nu} \cdot \left(1 - \frac{(t/3)^2}{2 \cdot Ra} \right) \cdot \left(\frac{Ra}{R} \right)^2 \right] \quad (1)$$

where F is the applied load, ν is the Poisson's ratio of the substrate material (here 0.32 for TZ), t is the sample thickness, Ra is the support radius, and R is the sample radius. One-way analysis of variance followed by Tukey's test (Minitab 16, Minitab Inc., State College, PA, USA) was performed for comparison of the biaxial flexural strength values between the different coated groups ($p \leq .05$). Additionally, fracture surfaces of the B3B specimens were examined with SEM to characterize the adhesion quality of the coating on the substrate.

Insertion of Zirconia Dental Implants

The prefabricated zirconia screws were split into two groups. One group ($n = 10$) was inserted into fresh bovine rib bone, and the second group ($n = 10$) was inserted into a biomechanical test block (solid rigid polyurethane foam [40 pcf = 0.64 g/cc]; Sawbones Europe AB, Malmö, Sweden). Drilling and insertion tools from the similarly macro designed implant system (BEGO Semados® RI; BEGO Implant Systems) were used. The insertion protocol followed the clinically proved sequence for the insertion of dental implants in patients, which was provided by the manufacturer's recommendations.

After insertion, the implants with surrounding bone tissue or polyurethane foam were embedded in resin (EpoFix, Struers GmbH, Willich, Germany) and grounded to the middle of the implant. After coating with a thin gold layer, the samples were examined with SEM.

RESULTS

Microstructure Characterization

Representative top views of the resulting microstructure observed by SEM after sintering at $1,500^\circ\text{C}$ are shown in Figure 2. The pore size, porosity, and thickness are compared in Table 3, as determined by image analysis of representative top views and cross sections and the average surface roughness of different coatings.

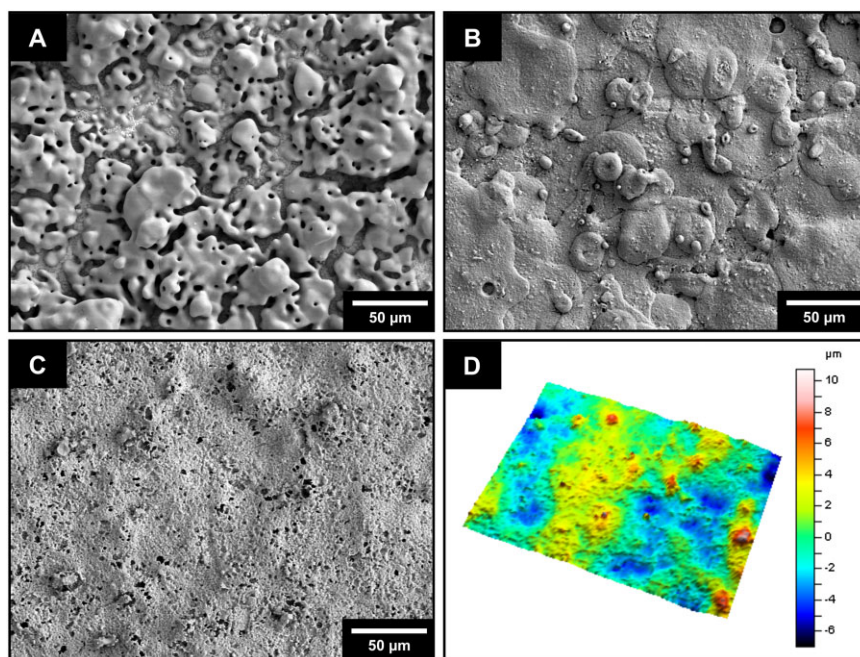


Figure 2 Surface morphology of different coatings on TZ obtained by WPS after sintering at 1,500°C. A, CP; B, TZ; C, TZCP; D, three-dimensional surface topography of TZCP.

As reference materials, pure CP and TZ coating were prepared. Both coatings displayed an inhomogeneous, irregular, and rough morphology. CP (Figure 2A) exhibited a lot of pores with different sizes varying from 2 to 30 μm , a porosity of 17.8% and an average roughness of $6.03 \pm 0.59 \mu\text{m}$. The height of the coating was around 16 μm . The formation of cracks along the coating surface was also detected, and the cracks had a width of less than 1.5 μm .

TZ samples (Figure 2B) in contrast showed almost no pores and splat morphology with some “donut” like structures. The average surface roughness was $3.46 \pm 0.45 \mu\text{m}$, and the coating thickness was about 20 μm . The coating featured a porosity of 1.6% with pore sizes varying between 1 and 15 μm .

The morphology of the zirconia/calcium phosphate coating (TZCP) (Figure 2C) composed of the starting

materials HA and TZ displayed an undulated and homogenous structure in terms of a fully covered surface with an average surface roughness of $3.54 \pm 0.40 \mu\text{m}$ and a thickness of around 23 μm . No cracks were present on the coating surface. Furthermore, pores of different sizes can be observed; the pore size varies from 1 to 15 μm , and the porosity was about 17.2%.

The average roughness of the uncoated substrate after sintering was $0.53 \pm 0.09 \mu\text{m}$, pointing out the significant increase of surface roughness after coating.

EDX Mapping and Phase Analysis

SEM images and the corresponding false color images of EDX elemental mapping are shown in Figure 3. Zirconium (Zr) is found in the coating and the substrate (Figure 3, B and E), whereas calcium (Ca) is only located in the coating (Figure 3, C and F). It can also be observed

TABLE 3 Properties of the Substrate and Sprayed Coatings

Sample Name	Roughness (Sa in μm)	Thickness (μm)	Pore Size (μm)	Porosity (%)
TZ uncoated	0.53 ± 0.09	1741 ± 12	1–2	1.3 ± 0.1
CP	6.03 ± 0.59	16.02 ± 5.52	2–30	17.8 ± 3.1
TZ	3.46 ± 0.45	20.14 ± 3.03	1–15	1.6 ± 0.2
TZCP	3.54 ± 0.40	22.59 ± 1.87	1–15	17.2 ± 2.4

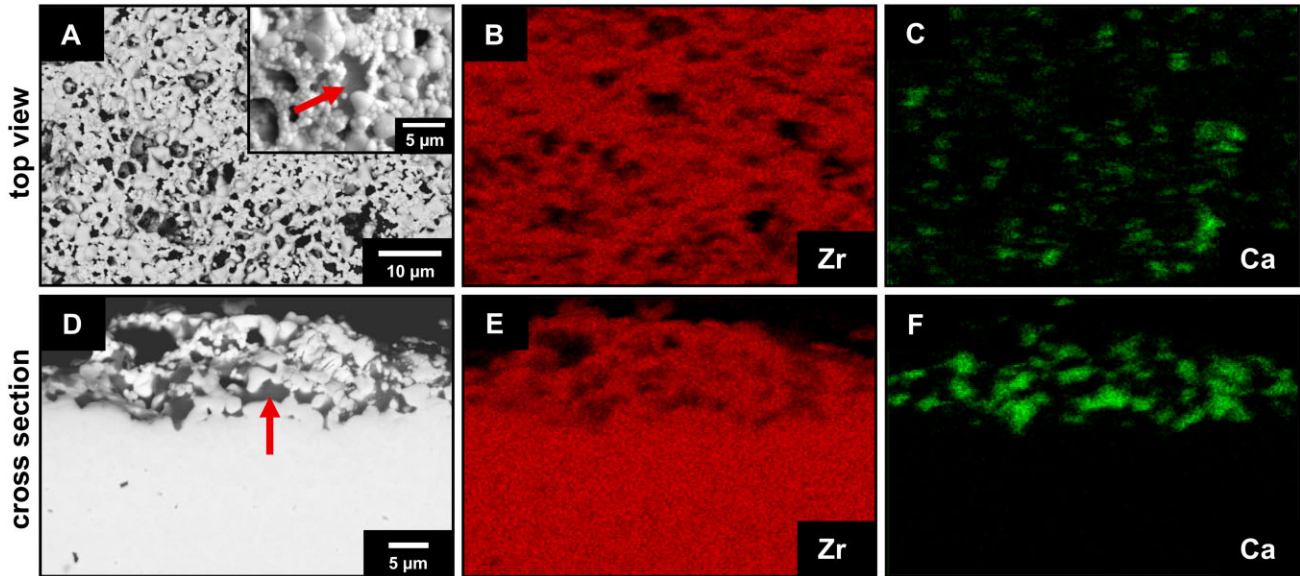


Figure 3 SEM micrographs of the mixed coating TZCP after sintering at 1,500°C and the corresponding EDX elemental mappings of Zr and Ca for the top view (A–C) and a polished cross-section (D–F). The red arrows point at dark gray areas that represent calcium phosphate regions.

that the calcium regions are equally distributed in the coating, indicating that neither vertical nor lateral sedimentation of TZ occurred after WPS. Higher magnifications of SEM micrographs (Figure 3, A and D) show two different areas in the mixed coating. Additional EDX point analyses (data not shown) depicted the typical peaks of Ca, phosphorus (P) and oxygen (O) in the dark gray areas and represent calcium phosphate regions (red arrows). Whereas measurements in the bright gray areas exhibited the typical peaks of Zr, Ca, and O, representing calcium stabilized zirconia regions.

To determine the phase composition of the different coatings, GI-XRD analyses were carried out after sintering and are shown in Figure 4. The top diffractogram exhibits the XRD pattern of TZCP that consisted of cubic calcium zirconium oxide ($\text{Ca}_{0.15}\text{Zr}_{0.85}\text{O}_{1.85}$), α -TCP, and monoclinic zirconia. For the pure CP coating, all peaks could be completely explained by β -TCP and α -TCP. The detected zirconia phase originates from the substrate. No change in phase composition was detected in the TZ coating after sintering. The main phase of TZ was tetragonal zirconia, and a negligible amount of the monoclinic phase was found in the GI-XRD pattern.

Characterization of the Coating Adhesion

The adhesion of the coating is one very important mechanical property of coated implants envisaged for load-bearing applications. Figure 5 illustrates the

coating surface before (Figure 5, A–C) and after the scratch test (Figure 5, D–I). The dashed black lines correspond to the pencil or bone scratch path. The pure CP coating (Figure 5, D and G) was completely damaged and largely removed indicating a poor coating adhesion to the substrate. In contrast, the results of the

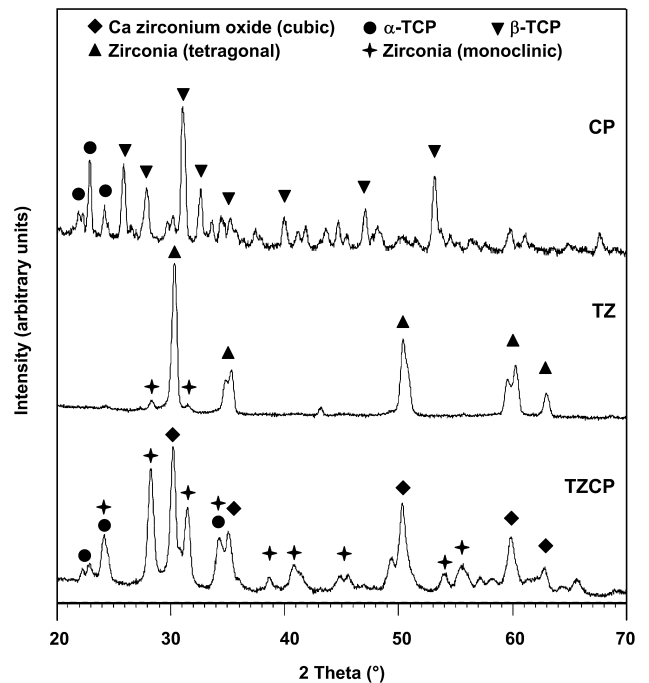


Figure 4 GI-XRD patterns of the CP, TZ, and TZCP coatings after heat treatment at 1,500°C with a dwell time of 2 hours.

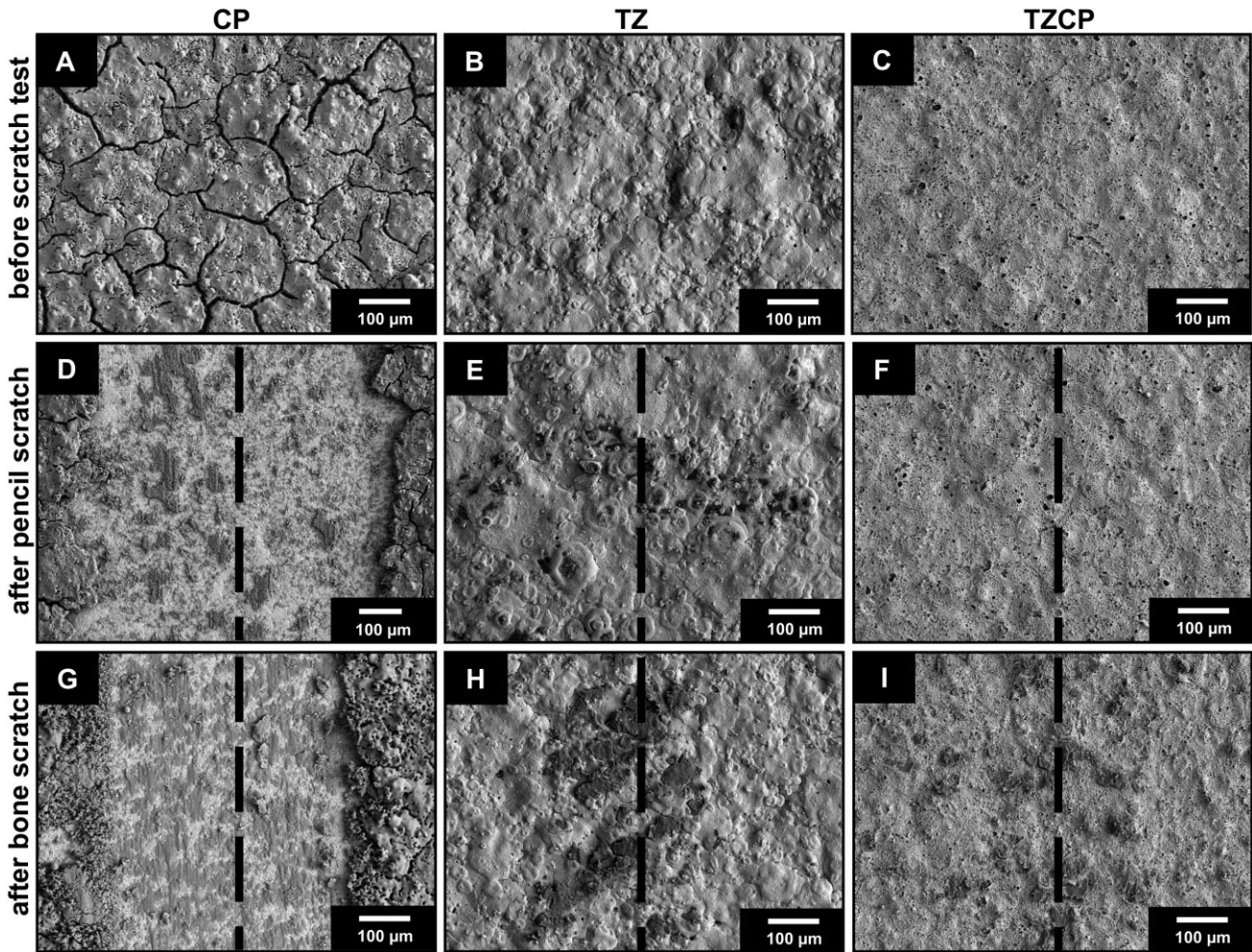


Figure 5 SEM micrographs of the adhesion testing via pencil scratch tester before (A–C) and after (D–I) the scratch test. The test was carried out with a pencil hardness grade of 9H on pure CP (D), pure TZ (E), and TZCP (F) and with bone on pure CP (G), pure TZ (H), and TZCP (I). The black dotted line represents the pencil and bone scratch path.

pure TZ (Figure 5, E and H) and mixed coating (Figure 5, F and I) showed no damage or removal of the coating induced by the pencil suggesting a firm attachment and a strong interbonding between the coating and the substrate.

Further investigations of fracture surfaces (Figure 6) confirm the scratch test results. The mixed (Figure 6C) and pure TZ coatings (Figure 6B) show a smooth and continuous morphology along the interbonding. Whereas on the CP coating (Figure 6A arrow),

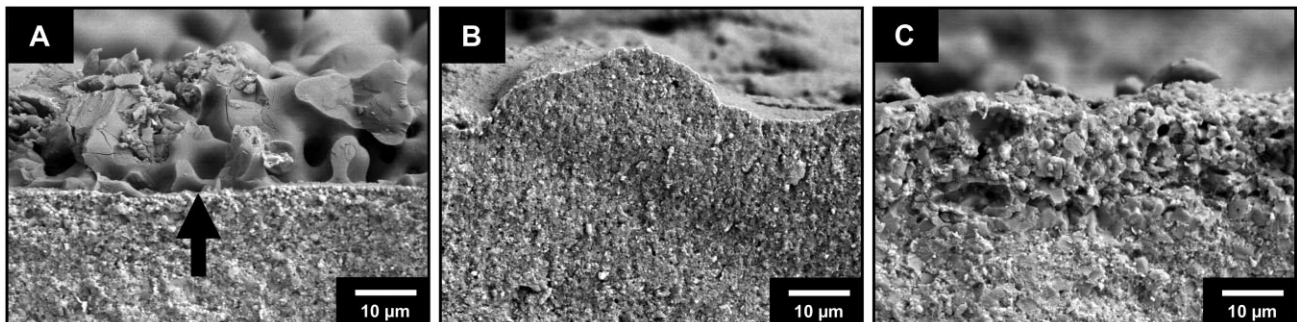


Figure 6 SEM micrographs of the fracture surfaces of CP (A), TZ (B), and TZCP (C) after heat treatment at 1,500°C. The arrow marks the interface between the coating and the substrate.

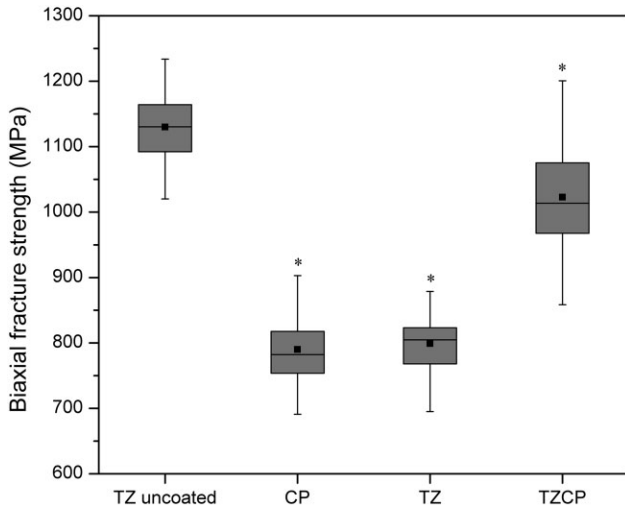


Figure 7 Box plot diagram depicting the biaxial strength of the different coated samples compared with an uncoated sample after sintering at 1,500°C. The box represents the spreading of the data between the 25th and 75th percentiles. The horizontal line in the box displays the median. The minimum and maximum values are illustrated by the whiskers. (■) marks the mean values. (*) $p < .05$ in comparison with the uncoated sample.

a distinct interface between the substrate and the coating could be observed. In some regions, a detachment of the coating was also visible (data not shown).

Characterization of the Biaxial Flexural Strength

The biaxial flexural strength of the coated samples was examined via B3B and compared with an uncoated TZ

substrate as shown in Figure 7. The mean strength value of the uncoated sample (TZ uncoated), CP, TZ, and TZCP were 1129.9 MPa, 789.9 MPa, 798.9 MPa and 1023.9 MPa, respectively. The highest strength value was observed for the uncoated sample (TZ); only a slight decrease in strength is shown for TZCP. In contrast, CP and TZ exhibited a significant decrease of strength compared with TZ and TZCP. In summary, it can be concluded that TZCP possesses the smallest impact on the overall strength of the samples within the various coatings.

Coating and Insertion of Complex Zirconia Dental Implants

Figure 8 shows a zirconia implant with a porous TZCP coating obtained by WPS. A homogeneously and fully coated implant (Figure 8A) was achieved. The detailed SEM image in Figure 8B reveals that the coating morphology is similar to that one obtained on the discs and features a coatings thickness of around 20 μm (Figure 8C).

The coated dental implants were inserted into polyurethane foam Sawbone and bovine rib bone to investigate the coating stability during implant placement (Figure 9, A and B). The SEM images depict the pure CP and TZCP coating after insertion followed by resin embedment. Samples coated with pure CP showed at the thread tips fully damaged coating (Figure 9, C and D). Dependent on the bone contact area, the thread sides

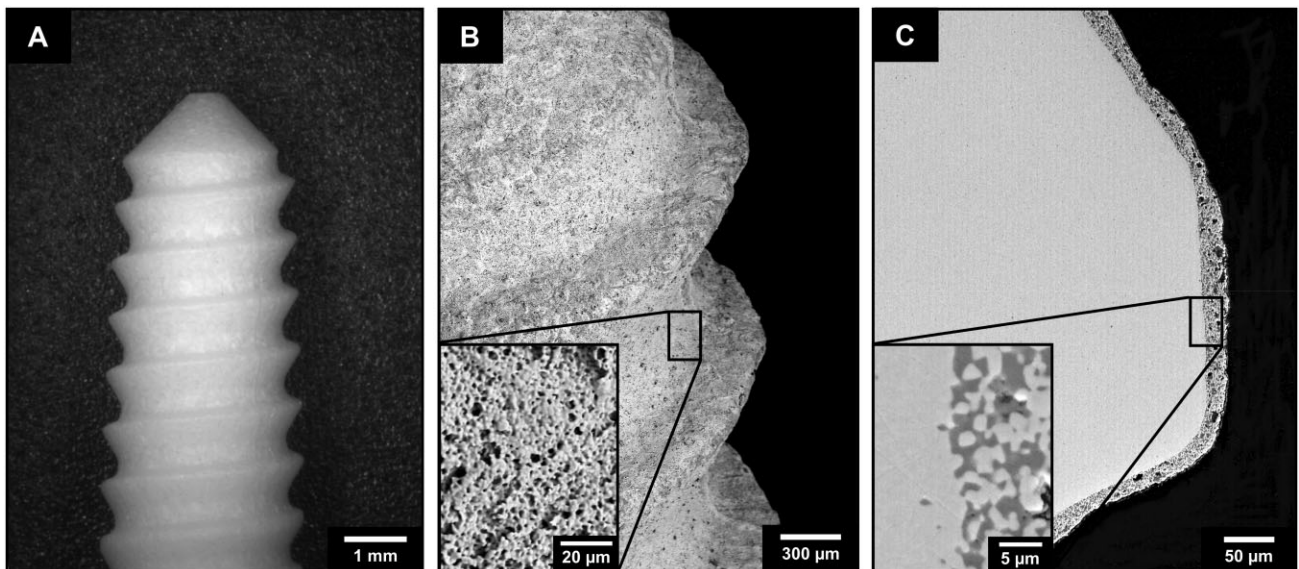


Figure 8 Implant overview (A), coating detail (B), and cross-section (C) of a zirconia implant coated with TZCP via WPS after sintering at 1,500°C.

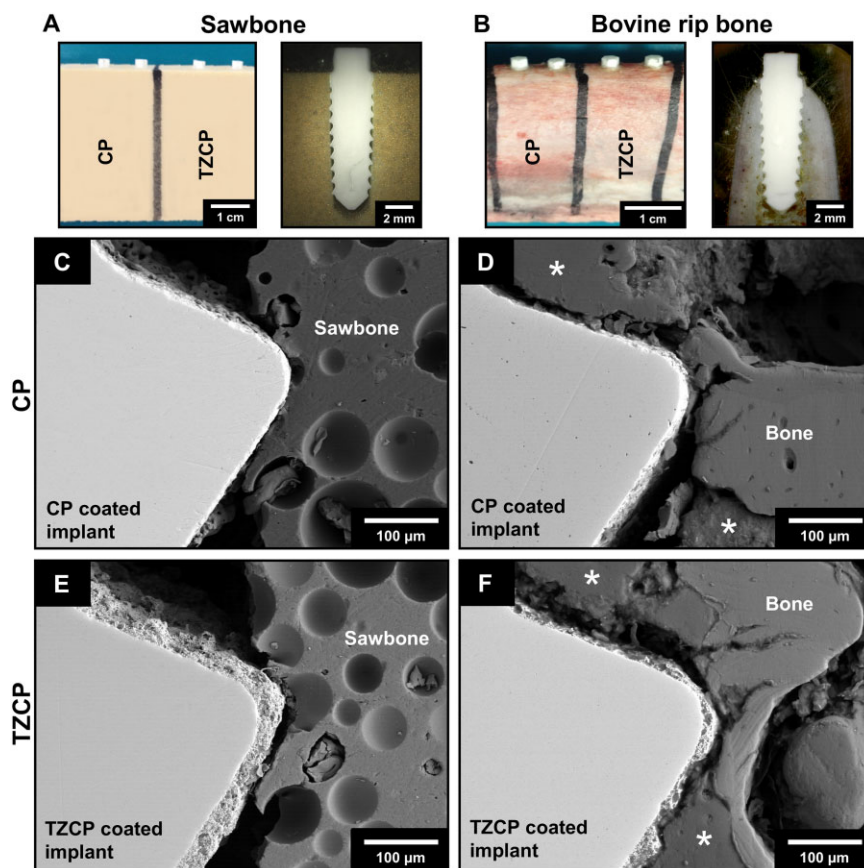


Figure 9 Coated TZ implants were inserted into polyurethane foam Sawbone (left column) and bovine rip bone (right column) using a clinical protocol. The coating adhesion was qualitatively characterized at the thread tips and sides of the pure CP coating (C and D) and TZCP (E and F) after embedding in resin. Asterisks indicate areas with residues of the polishing paste.

show a partial removal of the coating, which could also be partially caused by grinding. In the areas where the implant had no bone contact, the coating was still intact. In contrast, TZCP features a much higher coating stability; neither the insertion nor the grinding destroyed the coating (Figure 9, E and F), confirming the strong adhesion between substrate and coating. These findings are in accordance with the results from the scratch test (Figure 5).

DISCUSSION

The present study demonstrates the fabrication of a mixed coating on TZ, in order to increase the coating adhesion and stability. As a coating method, WPS was selected. WPS is a simple, environmental friendly and cost-effective method that has already been used successfully for the processing of porous coatings.^{30–32} Furthermore, it can easily be applied to deposit coatings with varying thicknesses on planar or curved surfaces.

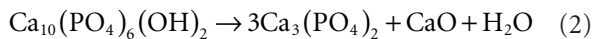
Coatings of CP and TZ were used as reference materials for comparative purposes with the mixed coating (TZCP). Therefore, suspensions were prepared with different solid contents to obtain various coatings with a comparable height and roughness. All prepared coatings displayed an irregular, rough, and porous surface morphology. Fully coated, crack-free surfaces for TZCP and TZ were obtained, whereas for CP cracks were observed. Furthermore, EDX analysis confirmed the uniformity of the TZCP coating; Zr and Ca were equally distributed in the coating layer.

The average surface roughness was evaluated, and TZCP and TZ showed the same roughness of around 4 μm ; only CP was slightly increased with 6 μm . In literature, surfaces with an average surface roughness of 4 to 7 μm were suggested to have a positive influence on long-term adhesion.^{33,34} The higher roughness resulted in mechanical interlocking and thus in an improved tissue integration.¹³ It is also known that osteoblastic cells are sensitive to different surface roughnesses.

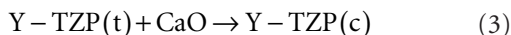
Usually, the cells possess a higher proliferation rate on smooth surfaces and a higher differentiation on rough surfaces.^{33,35,36} However, there is currently no consensus in literature about the appropriate roughness.

The porosity of the coating is another contributing factor to the long-term stability of an implant. While TZCP and CP showed a comparable porosity, TZ displayed a more dense structure with less pores. In consequence of the pores, an increased surface to volume ratio is reached and hence an increase of potential bone interface. It could be observed that the filopodia of osteoblasts appear to anchor pores of the coating, which may lead to a more efficient cell anchoring to the porous surface and therefore to a better adhesion of the cells to the material.³⁷ Furthermore, another concern in clinical research are possible inflammatory reactions after surgery caused by bacterial contamination. To avoid the removal of implants due to inflammatory reactions, porous coatings could be useful due to their higher loading capacity for antibacterial drugs. However, the pores can be also utilized to stimulate osteoblastic cells by loading them with, for example, growth factors, hormones, or enzymes.

The sintering after coating ensures a sufficient particle–particle and particle–substrate bonding; however, the high sintering temperature leads to phase transformations. The investigation of the TZCP GI-XRD pattern depicts that the HA fraction is decomposed during heat treatment to α -TCP, following Eq. 2.^{38,39}



The Ca ions from the HA decomposition diffuse into the zirconia phase and cause a transformation of tetragonal (t) to cubic (c); a calcium stabilized zirconia phase is obtained as described in Eq. 3.⁴⁰



The monoclinic phase in the mixed coating probably results from the excess of TZ, derived from the substrate. Normally, the formation of monoclinic zirconia in TZ/HA composites, where Y_2O_3 stabilized zirconia was used, will not occur; only tetragonal and cubic structure can be found.² These phase transformations were intentionally induced because of the higher degradation of tricalcium phosphate. TCP is a bioactive and bioresorbable ceramic that gradually dissolves within the body.

The faster release of Ca^{2+} and PO_4^{2-} ions in physiological fluids can stimulate bone formation. HA, in contrast, possesses a rather low degradation behavior in physiological environments, which could influence the optimal bone tissue formation. Therefore, the decomposition of HA to TCP does not represent a disadvantage for the biofunction.⁴¹ The pure CP coating without TZ transformed after sintering to β -TCP and α -TCP, indicating that similar reactions took place during heat treatment compared with the TZCP coating. The decomposition of HA into TCP at higher temperatures is well known and sufficiently investigated, with all its consequences such as the change of solubility.^{38,39} However, these circumstances will not be elucidated further in detail for the sake of simplicity; the pure CP coating has only been prepared for comparative purpose. TZ still remains tetragonal zirconia after sintering at 1,500°C.

The qualitative scratch test was performed under controlled load and speed by scratching the coated surfaces with specified pencil hardness and a sharpened bovine femur. TZCP and TZ showed no damage or removal of the coating, indicating enhanced adhesion strength. CP, in contrast, exhibited a weak resistance to the pencil and bone caused by the poor adhesion of the coating to the substrate. For the coating, presintered substrata were used; therefore, the opportunity for diffusion processes was given for particles of the substrate and the coating during temperature treatment, as solid-state sintering is a thermally activated process.⁴² Thus, the improved adhesion of the mixed coating may be attributed to the usage of presintered samples, the material mixture – where one part corresponds to the substrate – and the subsequent sintering step.

Analysis of fracture surfaces confirms the good adhesion of the mixed coating and TZ. The coating–substrate interface appears to be coherent and free of defects. No cracks or gaps appeared between the coating and the substrate in the specimens. The poor adhesion of the pure CP coating may be explained by the difference in thermal expansion coefficient of the coating ($13.3 \times 10^{-6}/\text{K}$)⁴³ and the substrate material ($10.8 \times 10^{-6}/\text{K}$).⁴⁴ This mismatch results in a weak attachment of the coating to the substrate. However, we are also aware of the fact that the microstructures of the prepared coatings are not comparable with 100% and could have an impact on the examined properties. However, one main focus of this study is the stability and

adhesion of the coating, and we believe that the material selection, the particle interactions, and the densification during the sintering process govern these properties.

The examination of the biaxial flexural strength revealed that TZCP exhibits almost the same strength as the uncoated sample. Therefore, it can be concluded that the strength of the sample is slightly affected by the presence of the mixed coating layer. In contrast, both CP and TZ show significant lower biaxial flexural strengths compared with the uncoated sample and TZCP. The results from the B3B test for CP and TZ emerge most likely from a combination of surface roughness and phase transformations at the interface. In CP, a higher amount of CaO is available that can diffuse into the zirconia substrate and cause a transformation from tetragonal to cubic. In contrast, in TZCP, most of the CaO is predominantly incorporated into the coating due to the excess of TZ. From literature, it is known that cubic zirconia has inferior mechanical properties compared with tetragonal zirconia due to the absence of the transformation toughening mechanism.² Probably the higher content of cubic phase at the interface of CP leads to the lower strength values. In TZ, it is most likely that the roughness has a great influence on the sample strength that leads to the insertion of stress peaks and thus to an earlier failure than uncoated TZ.⁴⁵ The influence of the coating thickness on the flexural strength can be neglected due to the comparable values between the different coatings.

When adopting the coating method for curved dental implants, the importance of the coating deposition on complex shaped components has to be considered. In this study, we could demonstrate the suitability of WPS for the production of homogenous, porous coatings on zirconia implants in order to increase the adhesion and mechanical stability of the coating. Therefore, we choose insertion studies to characterize the coating adhesion, as determinations of the tensile bond strength are not sufficient enough because of the porosity and roughness of the coatings. CP- and TZCP-coated specimens were inserted into polyurethane foam Sawbone and fresh bovine rib bone, respectively. Sawbone is a clinically relevant bone model material that provides reproducible and standardized experimental conditions.⁴⁶ Bovine rib bone, in contrast, exhibits a great similarity to jaw bone with its spongy bone structure beneath the cortical bone layer. With these insertion experiments, which are comparable with the

in vivo clinical situation, we could clearly show the increased bond strength of TZCP compared with a pure CP coating. The mixed coating was not damaged by the insertion, whereas the CP coating was only intact at the thread sides. These results indicate that TZCP-coated implants could reach a firm stability in bone.

Furthermore, with the WPS technology used in this study, it is also possible to carry out sequential coating steps to increase the coating thickness. The suspension composition can be varied, for example, by adding additives to increase the coating bioactivity. The solid loading of the suspension can also be altered to a certain amount due to the sprayability of the suspension (data not published). However, further studies are necessary to understand and to determine the bioactivity of the coating, the degradation behavior and kinetics of Ca and P ion release, as well as the detailed characterization of the coating properties in vitro and in vivo. In the latter, the long-term stability of the coating is of particular interest.

CONCLUSIONS

In this work, a mixed coating composed of calcium phosphate and zirconia has been successfully used to fabricate ceramic coatings on zirconia substrates by the WPS method and compared with a pure CP and pure TZ coating. Based on this technique, a porous coating with a roughness of about 4 μm , a pore size ranging from 1 to 15 μm , and a total porosity of $\sim 17\%$ were obtained for the mixed coating and were nearly identical to those values determined for CP and TZ. Our study revealed the same firm coating adhesion for the mixed coating compared with pure TZ coating and was much higher than the CP coating. Furthermore, the biaxial fracture strength showed almost the same strength as uncoated zirconia. Using the WPS method, our mixed coating was effectively applied on complex-shaped zirconia components with a great potential for dental implants. Future in vivo experiments should evaluate the histological reactions and clinical feasibility.

ACKNOWLEDGMENTS

We would like to acknowledge DFG (RE 2735/7-1) for the financial support. The authors are grateful to Petra Witte of Historische Geologie-Paläontologie, University Bremen, for implementation of the SEM and EDX analysis. We also thank Martin Ellerhorst from BEGO Implant Systems Bremen for providing the geometry of

the implants and Andreas Reindl from Fraunhofer IFAM Bremen for preparing and delivering the zirconia implants. We also would like to acknowledge Thomas Krause for fruitful discussions and Michael Teck for his help in the laboratory.

REFERENCES

- Niinomi M. Mechanical properties of biomedical titanium alloys. *Mater Sci Eng A* 1998; 243:231–236.
- Piconi C, Maccauro G. Zirconia as a ceramic biomaterial. *Biomaterials* 1999; 20:1–25.
- Chevalier J. What future for zirconia as a biomaterial? *Biomaterials* 2006; 27:535–543.
- Chevalier J, Gremillard L. Ceramics for medical applications: a picture for the next 20 years. *J Eur Ceram Soc* 2009; 29:1245–1255.
- Conrad HJ, Seong WJ, Pesun GJ. Current ceramic materials and systems with clinical recommendations: a systematic review. *J Prosthet Dent* 2007; 98:389–404.
- Manicone PF, Iommetti PR, Raffaelli L. An overview of zirconia ceramics: basic properties and clinical applications. *J Dent* 2007; 35:819–826.
- Att W, Hori N, Takeuchi M, et al. Time-dependent degradation of titanium osteoconductivity: an implication of biological aging of implant materials. *Biomaterials* 2009; 30:5352–5363.
- Balasundaram G, Webster TJ. Increased osteoblast adhesion on nanograined Ti modified with KRSR. *J Biomed Mater Res* 2007; 80A:602–611.
- Hempel U, Thomas H, Marie K, Cornelia W-B, Peter D, Falko S. Response of osteoblast-like SAOS-2 cells to zirconia ceramics with different surface topographies. *Clin Oral Implants Res* 2009; 21:174–181.
- Hao L, Lawrence J, Chian KS. Osteoblast cell adhesion on a laser modified zirconia based bioceramic. *J Mater Sci Mater Med* 2005; 16:719–726.
- Delgado-Ruiz RA, Calvo-Guirado JL, Moreno P, et al. Femtosecond laser microstructuring of zirconia dental implants. *J Biomed Mater Res B* 2011; 96B:91–100.
- Borsari V, Giavaresi G, Fini M, et al. Physical characterization of different-roughness titanium surfaces, with and without hydroxyapatite coating, and their effect on human osteoblast-like cells. *J Biomed Mater Res B* 2005; 75B:359–368.
- Le Guéhennec L, Soueidan A, Layrolle P, Amouriq Y. Surface treatments of titanium dental implants for rapid osseointegration. *Dent Mater* 2007; 23:844–854.
- Guo L, Li H. Fabrication and characterization of thin nano-hydroxyapatite coatings on titanium. *Surf Coat Tech* 2004; 185:268–274.
- Kim H-W, Georgiou G, Knowles JC, Koh Y-H, Kim H-E. Calcium phosphates and glass composite coatings on zirconia for enhanced biocompatibility. *Biomaterials* 2004; 25:4203–4213.
- Miao X, Hu Y, Liu J, Huang X. Hydroxyapatite coating on porous zirconia. *Mater Sci Eng C* 2007; 27:257–261.
- Dorozhkin SV. Calcium orthophosphates in nature, biology and medicine. *Materials* 2009; 2:399–498.
- Sampathkumaran U, De Guire MR, Wang R. Hydroxyapatite coatings on titanium. *Adv Eng Mater* 2001; 3:401–405.
- Zhang Y, Fu T, Han Y, Wang Q, Zhao Y, Xu K. In vitro and in vivo tests of hydrothermally synthesised hydroxyapatite coating. *Biomol Eng* 2002; 19:57–61.
- Jarcho M. Calcium phosphate ceramics as hard tissue prosthetics. *Clin Orthop* 1981; 157:259–278.
- Hench LL. Bioceramics – from concept to clinic. *J Am Ceram Soc* 1991; 74:1487–1510.
- Baltag I, Watanabe K, Kusakari H, et al. Long-term changes of hydroxyapatite-coated dental implants. *J Biomed Mater Res* 2000; 53:76–85.
- Best SM, Porter AE, Thian ES, Huang J. Bioceramics: past, present and for the future. *J Eur Ceram Soc* 2008; 28:1319–1327.
- Matsumoto TJ, An S-H, Ishimoto T, Nakano T, Matsumoto T, Imazato S. Zirconia-hydroxyapatite composite material with micro porous structure. *Dent Mater* 2011; 27:e205–e212.
- Yugeswaran S, Yoganand CP, Kobayashi A, Paraskevopoulos KM, Subramanian B. Mechanical properties, electrochemical corrosion and in-vitro bioactivity of yttria stabilized zirconia reinforced hydroxyapatite coatings prepared by gas tunnel type plasma spraying. *J Mech Behav Biomed Mater* 2012; 9:22–33.
- Bao-Chyi W, Edward C, Chyun-Yu Y. Characterization of plasma-sprayed bioactive hydroxyapatite coatings in vitro and in vivo. *Mater Chem Phys* 1994; 37:55–63.
- Gadow R, Killinger A, Stiegler N. Hydroxyapatite coatings for biomedical applications deposited by different thermal spray techniques. *Surf Coat Tech* 2010; 205:1157–1164.
- Kim HW, Kong YM, Bae CJ, Noh YJ, Kim HE. Sol-gel derived fluor-hydroxyapatite biocoatings on zirconia substrate. *Biomaterials* 2004; 25:2919–2926.
- Wu C, Ramaswamy Y, Gale D, et al. Novel sphenic coatings on Ti-6Al-4V for orthopedic implants using sol-gel method. *Acta Biomater* 2008; 4:569–576.
- Ruder A, Buchkremer HP, Jansen H, Malléner W, Stöver D. Wet powder spraying – a process for the production of coatings. *Surf Coat Tech* 1992; 53:71–74.
- Buchkremer HP, Menzel NH. Coating technologies. In: Groza JR, Shackelford JF, Lavernia EJ, Powers MT, eds. *Materials processing handbook*. Boca Raton, FL: CRC Press, 2007: 24.10–24.26.
- Zhou W, Shi H, Ran R, Cai R, Shao Z, Jin W. Fabrication of an anode-supported yttria-stabilized zirconia thin film for solid-oxide fuel cells via wet powder spraying. *J Power Sources* 2008; 184:229–237.

33. Bächle M, Kohal RJ. A systematic review of the influence of different titanium surfaces on proliferation, differentiation and protein synthesis of osteoblast-like MG63 cells. *Clin Oral Implants Res* 2004; 15:683–692.
34. Boyan BD, Lössdorfer S, Wang L, et al. Osteoblasts generate an osteogenic microenvironment when grown on surfaces with rough microtopographies. *Eur Cell Mater* 2003; 6:22–27.
35. Boyan BD, Lohmann CH, Dean DD, Sylvia VL, Cochran DL, Schwartz Z. Mechanisms involved in osteoblast response to implant surface morphology. *Annu Rev Mater Res* 2001; 31:357–371.
36. Anselme K. Osteoblast adhesion on biomaterials. *Biomaterials* 2000; 21:667–681.
37. Briggs EP, Walpole AR, Wilshaw PR, Karlsson M, Palsgard E. Formation of highly adherent nano-porous alumina on Ti-based substrates: a novel bone implant coating. *J Mater Sci Mater Med* 2004; 15:1021–1029.
38. Evis Z, Sato M, Webster TJ. Increased osteoblast adhesion on nanograined hydroxyapatite and partially stabilized zirconia composites. *J Biomed Mater Res A* 2006; 78A:500–507.
39. Zhang JX, Iwasa M, Kotobuki N, et al. Fabrication of hydroxyapatite-zirconia composites for orthopedic applications. *J Am Ceram Soc* 2006; 89:3348–3355.
40. Evis Z, Usta M, Kutbay I. Hydroxyapatite and zirconia composites: effect of MgO and MgF₂ on the stability of phases and sinterability. *Mater Chem Phys* 2008; 110:68–75.
41. Uchino T, Yamaguchi K, Suzuki I, Kamitakahara M, Otsuka M, Ohtsuki C. Hydroxyapatite formation on porous ceramics of alpha-tricalcium phosphate in a simulated body fluid. *J Mater Sci Mater Med* 2010; 21:1921–1926.
42. Lhermitte-Sebire I, Colmet R, Naslain R, Desmaison J, Gladel G. The adhesion between physically vapour-deposited or chemically vapour-deposited alumina and TiC-coated cemented carbides as characterized by Auger electron spectroscopy and scratch testing. *Thin Solid Films* 1986; 138:221–233.
43. Jiang G, Shi D. Coating of hydroxyapatite on highly porous Al₂O₃ substrate for bone substitutes. *J Biomed Mater Res* 1998; 43:77–81.
44. Hayashi H, Saitou T, Maruyama N, Inaba H, Kawamura K, Mori M. Thermal expansion coefficient of yttria stabilized zirconia for various yttria contents. *Solid State Ionics* 2005; 176:613–619.
45. Zheng Y, Vieira JM, Oliveira FJ, Davim JP, Brogueira P. Relationship between flexural strength and surface roughness for hot-pressed Si₃N₄ self-reinforced ceramics. *J Eur Ceram Soc* 2000; 20:1345–1353.
46. Schneider M, Loukota R, Reitemeier B, et al. Bone block fixation by ultrasound activated resorbable pin osteosynthesis: a biomechanical in vitro analysis of stability. *Oral Surg Oral Med Oral Pathol Oral Radiol Endod* 2010; 109: 79–85.

Copyright of Clinical Implant Dentistry & Related Research is the property of Wiley-Blackwell and its content may not be copied or emailed to multiple sites or posted to a listserv without the copyright holder's express written permission. However, users may print, download, or email articles for individual use.